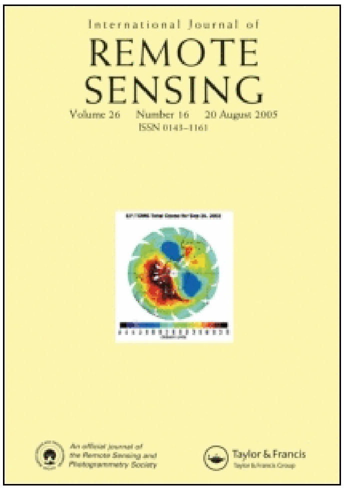

International Journal of Remote Sensing
Publication details, including instructions for authors and subscription information:
http://www.informaworld.com/smpp/title~content=t713722504

Evaluation of SeaWiFS and MODIS chlorophyll-a products in the Argentinean Patagonian Continental Shelf (38° S-55° S)

A. I. Dogliotti [ab]; I. R. Schloss [bc]; G. O. Almandoz [bd]; D. A. Gagliardini [abe]
[a] Instituto de Astronomía y Física del Espacio (IAFE-CONICET), Pabellón IAFE-Ciudad Universitaria, C.C. 67-sucursal 28 (1428) Buenos Aires, Argentina [b] Consejo Nacional de Investigaciones Científicas y Técnicas, Argentina [c] Instituto Antártico Argentino, Cerrito 1248 (1010) Ciudad de Buenos Aires, Argentina [d] Facultad de Ciencias Naturales y Museo, Universidad Nacional de La Plata, La Plata, Argentina [e] Centro Nacional Patagónico (CENPAT-CONICET), Puerto Madryn, Argentina

Online Publication Date: 01 January 2009

To cite this Article Dogliotti, A. I., Schloss, I. R., Almandoz, G. O. and Gagliardini, D. A.(2009)'Evaluation of SeaWiFS and MODIS chlorophyll-a products in the Argentinean Patagonian Continental Shelf (38° S-55° S)',International Journal of Remote Sensing,30:1,251 — 273

To link to this Article: DOI: 10.1080/01431160802311133

URL: http://dx.doi.org/10.1080/01431160802311133

International Journal of Remote Sensing
Vol. 30, No. 1, 10 January 2009, 251–273

Taylor & Francis
Taylor & Francis Group

Evaluation of SeaWiFS and MODIS chlorophyll-*a* products in the Argentinean Patagonian Continental Shelf (38° S–55° S)

A. I. DOGLIOTTI*†‡, I. R. SCHLOSS‡§, G. O. ALMANDOZ‡¶ and D. A. GAGLIARDINI†‡||

†Instituto de Astronomía y Física del Espacio (IAFE-CONICET), Pabellón IAFE-Ciudad Universitaria, C.C. 67-sucursal 28 (1428) Buenos Aires, Argentina
‡Consejo Nacional de Investigaciones Científicas y Técnicas, Argentina
§Instituto Antártico Argentino, Cerrito 1248 (1010) Ciudad de Buenos Aires, Argentina
¶Facultad de Ciencias Naturales y Museo, Universidad Nacional de La Plata, Paseo del Bosque s/n (1900), La Plata, Argentina
||Centro Nacional Patagónico (CENPAT-CONICET), Boulevard Brown s/n, Puerto Madryn, Argentina

(*Received 20 April 2007; in final form 26 June 2008*)

Field measurements of surface chlorophyll-*a* concentration were used to evaluate for the first time the performance of the standard Moderate Resolution Imaging Spectroradiometer (MODIS) and both standard and regional Sea-viewing Wide Field-of-view Sensor (SeaWiFS) ocean colour algorithms in the Patagonian Continental Shelf (PCS) between 38° S and 55° S. The results showed that the regional algorithms did not significantly improve the global algorithm estimates. Moreover, the SeaWiFS OC4v4 algorithm, National Aeronautics and Space Administration (NASA) standard chlorophyll product, showed the best performance among all the algorithms examined. Nonetheless, all the global and local algorithms analysed showed uncertainties dependent on chlorophyll concentration. Low chlorophyll-*a* concentration values tended to be overestimated and high values tended to be underestimated. A regional analysis within the PCS showed that higher uncertainties are found in the homogeneous side of the tidal fronts present in the PCS, in areas suggested to be optically complex case 2 waters, while a better result (less bias) was obtained in the southern mid-shelf region. We discuss the probable reasons and provide possible explanations of the regional differences in the performance of the algorithms.

1. Introduction

Remote sensing of ocean-colour data has demonstrated to be a very useful tool in monitoring the marine ecosystem. It has provided near real-time, long-term, synoptic, global estimates of key parameters, such as surface chlorophyll (as an index of phytoplankton biomass), that can be integrated in basin-scale models such as primary production models (Longhurst *et al.* 1995, Behrenfeld and Falkowski 1997). However, uncertainties in remote sensing retrievals can arise from sensor calibration, atmospheric correction and bio-optical algorithms; the presence of clouds further limits its use, especially at high latitudes. Moreover, the estimates of phytoplankton biomass correspond to the upper layer of the water column (first

*Corresponding author. Email: adogliotti@iafe.uba.ar

International Journal of Remote Sensing
ISSN 0143-1161 print/ISSN 1366-5901 online © 2009 Taylor & Francis
http://www.tandf.co.uk/journals
DOI: 10.1080/01431160802311133

optical depth) and extrapolation from surface chlorophyll concentrations to vertical chlorophyll profiles is required by the primary production models (Sathyendranath *et al.* 2000). In spite of the mentioned limitations and uncertainties, satellite observations of the ocean provide invaluable information for biological, ecological and oceanographic applications at basin and global scales.

Since the launch of the first ocean colour sensor, the Coastal Zone Colour Scanner (CZCS) in 1978, and the subsequent and more advanced ocean colour instruments (such as the Ocean Colour and Temperature Scanner (OCTS), the Sea-Viewing Wide Field-of-view Sensor (SeaWiFS), the MODerate resolution Imaging spectroradiometer (MODIS) and the MEdium Resolution Imaging Spectrometer (MERIS)), global algorithms have been empirically derived from a large *in situ* database collected in waters around the world (O'Reilly *et al.* 1998, 2000, Morel and Antoine 2007). These empirical algorithms rely on mean statistical relationship between chlorophyll-*a* concentration (Chl-*a*) and the blue-to-green reflectance ratio, and hold true in case 1 waters according to the bipartite classification scheme introduced by Morel and Prieur (1977). In these typically oceanic waters, the optical properties are exclusively controlled by phytoplankton and their associated materials (such as debris, heterotrophic organisms and bacteria, and dissolved organic matter released by these organisms). The presence of phytoplankton with a pigment composition different from the one used to build the empirical algorithms may cause the empirical relationship to break down. Furthermore, deviations from standard relationships could be caused by the presence of optically active components other than chlorophyll that can either co-vary or not co-vary with chlorophyll concentration. The empirical relationship will not hold even in cases where these substances do co-vary with Chl-*a* but, at different proportions than the ones used in the original dataset. These optically active substances can be dissolved or particulate materials from terrestrial origin, re-suspended from the bottom in shallow waters, or brought by land drainage and runoff. Global algorithms perform well in some regions of the world, especially where the *in situ* data were obtained to build the algorithms (Bailey *et al.* 2000, Hooker and McClain 2000). However, some authors find that more regional algorithms generally perform better, since they take into account the local biological characteristics of the region (e.g. Darecki *et al.* 2005, Volpe *et al.* 2007). The first attempts for SeaWiFS regional algorithms over the southwestern Atlantic Ocean were provided by Garcia *et al.* (2005, 2006). The two regional algorithms therein presented showed better performance than the global empirical and semi-analytical algorithms analysed.

The relatively flat continental shelf located in the south western Atlantic Ocean, south of approximately 40° S, is generally referred as the Patagonian Continental Shelf (PCS). It is delimited by the Patagonian coast to the west, and by the shelf break to the east (closely following the 200 m isobath), and its width ranges from ~210 km at 38° S to ~850 km at 52° S (figure 1). The PCS surface circulation is mainly dominated by local westerly and south-westerly winds. Oceanic and coastal fronts, as well as freshwater inputs from several Patagonian rivers and by the inflow of diluted waters from the Magellan Strait additionally influence the PCS circulation (Forbes and Garrafo 1988, Glorioso and Flather 1997, Piola and Rivas 1997). In a recent study Bianchi *et al.* (2005) found that the mid-shelf PCS waters act as a sink of CO_2 and that it was associated with high Chl-*a* values. Subsequently, Schloss *et al.* (2007) suggested that phytoplankton production could have greatly influenced the negative average ΔpCO_2 values (i.e. the difference between CO_2 concentration in

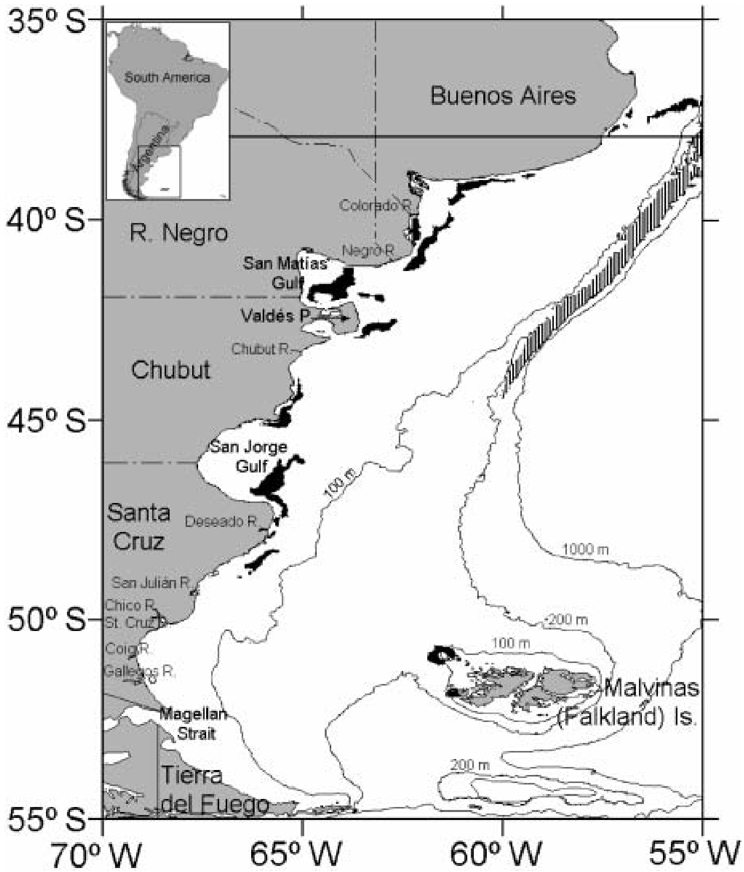

Figure 1. Area of study, the Patagonian Continental Shelf (PCS) between 38° S to 55° S. January mean surface thermal fronts (surface gradient $>0.25°C\ km^{-1}$) are shown over the PCS: black areas depict tidal coastal fronts and hatched area the shelf-break front (adapted from Bava *et al.* (2000)). Contours correspond to the 100, 200 and 1000 m isobaths. Local names used in the text and major rivers are also indicated.

the sea and in the atmosphere) found in this area, confirming the importance of the continental shelf and slope in the carbon cycle.

Previous studies used SeaWiFS data to examine the spatial and temporal Chl-*a* variability in the PCS, the Brazil–Malvinas Current Confluence region and the open ocean (Podestá 1997, Garcia *et al.* 2004, Gonzales-Silvera *et al.* 2004, Saraceno *et al.* 2005, 2006, Rivas 2006, Rivas *et al.* 2006, Lutz *et al.* 2006, Romero *et al.* 2006). In contrast, fewer studies have been made using MODIS data (Barré *et al.* 2006). A first validation of SeaWiFS-derived chlorophyll was performed by Armstrong *et al.* (2004) in the Río de La Plata estuary and adjacent waters. It showed that the OC2v2 SeaWiFS Chl-*a* algorithm significantly overestimated near-surface Chl-*a* in the Río de la Plata turbid waters (up to six times), but provided adequate estimates (within 10%) in the subtropical clear waters of the Brazil Current. Recently, a comparison of satellite-derived versus *in situ* measurements performed at 'Estación Permanente de Estudios Ambientales' (EPEA), a coastal station located south of Buenos Aires Province (figure 1), showed that, in general, OC4v4 estimates are in good agreement with *in situ* bio-optical observations (Lutz *et al.* 2006). However, a more regional comparison of satellite-derived and *in situ* data in the whole PCS has not been performed.

The main objective of the present work is to quantify the accuracy of global and regional empirical algorithms over the PCS and to further identify the possible causes when the algorithms fail. In particular, attention will be given to the specific composition of the phytoplankton community.

2. Data and methods

2.1 *In situ Chl-a*

In situ Chl-*a* measurements were performed during five field campaigns carried out in the Argentinean Continental Shelf off Patagonia through the years 2001–2004 (table 1) on board the icebreaker 'Almirante Irizar' in the frame of an Argentinean–French cooperative research ('ARGAU', for further details see Balestrini *et al.* (2000)). The locations of the stations are reported in figure 2(*a*). The samples were collected from the continuous water pumping system, located 9 m below the surface, every three hours all along the ship track. During each cruise, 2 to 4 l of seawater were filtered onto GF/F filters as well as onto 5 and 10 µm polycarbonate filters. All filters were frozen at -20°C until analysis at the Instituto Antártico Argentino. 90% acetone pigment extracts were read in a Beckman DU 650 spectrophotometer. Total Chl-*a* values were corrected for phaeopigments. Chl-*a* concentrations were calculated after Strickland and Parsons (1972). The final precision for Chl-*a* is 0.05 mg m^{-3}. Data of the 2002 cruise were not used since they were not corrected for phaeopigments.

2.2 *Microscopic analysis*

Both net (20 µm mesh) and quantitative samples were collected directly from the pumping system for phytoplankton analyses. All samples were fixed with acidic Lugol's iodine solution and kept in dark conditions at room temperature until analysis at the phycology laboratory of La Plata University. Net samples were observed by light microscopy both in water mounts and in oxidized material mounted in Naphrax with a phase contrast Wild M20 microscope, and were additionally examined by scanning electron microscopy (Jeol JSM-6360 LV, at the SEM service, Museo de La Plata). Cells were enumerated with an Iroscope SI-PH inverted microscope according to the procedures described by Utermöhl (1958). Approximately 400 cells were counted to obtain an estimate of the cell concentration with a precision of $\pm 10\%$ (Andersen and Throndsen 2003).

Table 1. Cruises to the Patagonian Continental Shelf.

Cruise name	Period	Season
ARGAU-01	5 January–21 February 2001	Summer
	5–8 April 2001	Autumn
ARGAU-01i	8–24 August 2001	Winter
ARGAU-03	7–10 February 2003	Summer
	15–19 May 2003	Autumn
ARGAU-04	27 February–16 March 2004	Summer
	14–18 April 2004	Autumn
ARGAU-05	25–28 December 2004	Spring

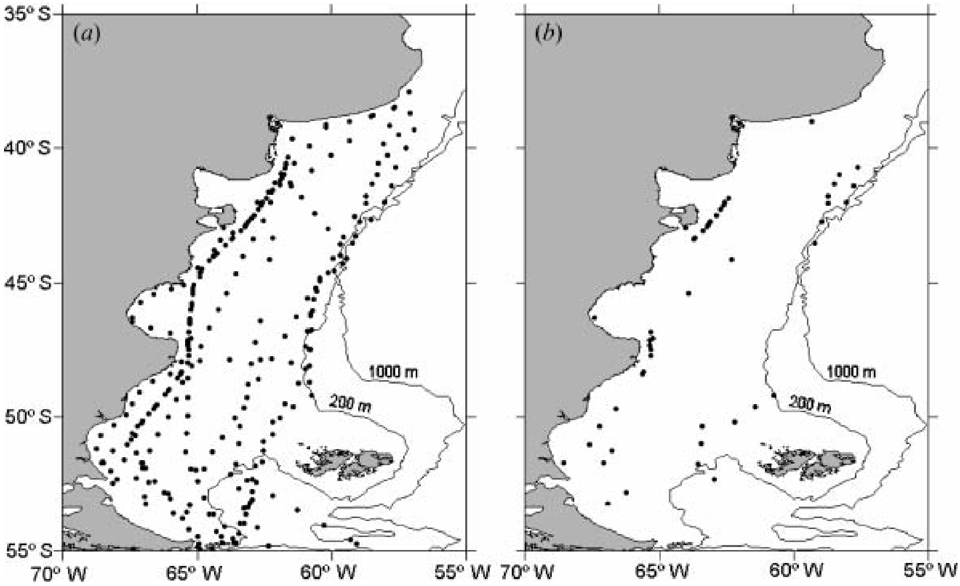

Figure 2. (*a*) Location of *in situ* Chl-*a* data collected during ARGAU campaigns. (*b*) Location of satellite and *in situ* match-ups data using the temporal criteria selected (± 3 h window around the satellite overpass). Contours correspond to the 200 and 1000 m isobaths.

2.3 *Satellite data*

SeaWiFS and MODIS/Aqua level 1A and ancillary data on ozone concentration and meteorological conditions (wind speed, oxygen concentration, water vapour and atmospheric pressure) were obtained from the NASA Distributed Active Archive Center (DAAC) for the days where coincident *in situ* data were available. SeaWiFS local area coverage (LAC) full resolution imagery was considered for the evaluation of the products. The selected images were processed to level 2 and the data products obtained were: Chl-*a* products, normalized spectral water-leaving radiance ($nL_w(\lambda)$), aerosol optical thickness at 865 nm ($\tau_a(865)$), as well as ancillary information such as solar and sensor zenith angles and L2 processing flags. The SeaWiFS Data Analysis System (SeaDAS) version 4.8 (update #4) software (Baith *et al.* 2001) was used and the products were mapped to a cylindrical equidistant projection at ~1 km spatial resolution at nadir. The standard atmospheric correction scheme used ('msl12' version 5.3.3) incorporates techniques that avoid the black pixel assumption. Although the present near infrared (NIR) correction procedure generally improves the satellite retrievals, overcorrection of the water-leaving radiance spectra in the blue region may still occur in turbid coastal waters, and overestimation of Chl-*a* and reduction of the algorithm's performance are expected in these regions.

In addition, SeaWiFS level 2 global area coverage (GAC) data were obtained from the DAAC and mapped to a cylindrical equidistant projection at 4 km resolution. Seasonal averages were used for the spatial distribution analysis of case 1/case 2 waters using the Lee and Hu (2006) criterion.

2.4 *Match-up procedure*

The pixels that were located nearest to the *in situ* locations in each available image were identified. *In situ* data were collected every three hours independently of the satellite time overpass. In order to define the temporal coincidence between satellite and *in situ* measurements, a temporal threshold was chosen. In this study, we considered a ± 3 h window around the satellite overpass, assuming that illumination is sufficient and atmospheric conditions are stable over this period (Bailey *et al.* 2000). A 3×3 window centred at the location of each station was defined to minimize georeference errors and statistics were computed for each window (mean and standard deviation) in order to evaluate the spatial stability or homogeneity at each station.

2.5 *Excluding criteria*

To minimize the effect of bad data on the comparison, a set of exclusion criteria was used. Pixels where the viewing and solar zenith angles were higher than 60° and 70°, respectively, were excluded. This exclusion takes into account that at extreme viewing and solar angles the atmospheric correction is less accurate (Ding and Gordon 1994). The L2 processing flags were used to exclude questionable pixels. Pixels were masked and not considered in the analysis if any of the standard flags of the processing code (Bailey and Werdell 2006) were set, i.e. atmospheric correction failure, pixel over land, high sun glint, total radiance above the knee value, high sensor and solar zenith angles, stray light on scene, cloud/ice and low normalized water-leaving radiance at 555 or 551 nm. A minimum number of valid pixels (not flagged), 5 out of 9 pixels in the 3×3 window, should be valid in order to rely on the mean value computed, thus avoiding erroneous retrievals. Furthermore, the coefficient of variation (CV) was computed for the Chl-*a* values within each 3×3 window and the retrieved value was excluded if the CV$\geqslant$0.2. This was carried out in order to avoid strong variation within each window, evidencing non-homogeneous regions.

3. Evaluating SeaWiFS and MODIS Chl-*a*

Satellite-derived Chl-*a* was computed using five empirical algorithms. Two global (OC2v4 and OC4v4) and two regional (OC2-LP and OC4-F) products were computed for SeaWiFS, and the standard OC3M product was processed for MODIS/Aqua (table 2). To quantify the uncertainties on the satellite-derived Chl-*a* products in the PCS, we compared the mentioned five products with *in situ* spectrophotometric measurements.

Statistical and graphical criteria were used to evaluate the agreement between Chl-*a* estimated by different algorithms and *in situ* measured Chl-*a* concentrations. Before statistical analysis was performed and in order to compare the different algorithms analysed, *in situ* and satellite-derived data were logarithmically transformed, given that bio-optical data tend to be log-normally distributed (Campbell 1995). Thus, the algorithm retrieval error was estimated as the difference between log-transformed values of predicted and measured chlorophyll concentrations. The statistics used to compare different algorithms were the mean error (BIAS-log) and the root mean square logarithmic error (RMS-log), both of which have been recently used in the literature (O'Reilly *et al.* 2000, Darecki *et al.* 2005). These errors were calculated using the following equations:

$$\text{BIAS-log} = \frac{1}{n}\sum\left[\log_{10}(C_{\text{sat}}) - \log_{10}(C_{\text{situ}})\right] \quad (1)$$

Table 2. Maximum band ratio algorithms for the SeaWiFS and MODIS sensors.

Sensor	Name	Equation
SeaWiFS	OC2v4	$\text{Chl-}a = 10^{\left(0.319-2.336R+0.879R^2-0.135R^3\right)}-0.071$ where $R=\log_{10}(R_{rs}(490)/R_{rs}(555))$
	OC4v4	$\text{Chl-}a = 10^{\left(0.366-3.067R+1.93R^2+0.649R^3-1.532R^4\right)}$ where $R=\log_{10}((R_{rs}(443)>R_{rs}(490)>R_{rs}(510))/R_{rs}(555))$
	OC4-F	$\text{Chl-}a = 10^{\left(0.277-3.192R+7.446R^2-12.035R^3+5.811R^4\right)}$ where $R=\log_{10}((R_{rs}(443)>R_{rs}(490)>R_{rs}(510))/R_{rs}(555))$
	OC2-LP	$\text{Chl-}a = 10^{\left(0.1691-1.8562R+0.6372R^2-1.6266R^3\right)}$ where $R=\log_{10}(R_{rs}(490)/R_{rs}(555))$
MODIS	OC3M	$\text{Chl-}a = 10^{\left(0.283-2.753R+1.457R^2-0.659R^3-1.403R^4\right)}$ where $R=\log_{10}((R_{rs}(443)>R_{rs}(488))/R_{rs}(550))$

and

$$\text{RMS-log} = \sqrt{\frac{1}{n}\sum\left[\log_{10}(C_{sat})-\log_{10}(C_{situ})\right]^2}, \tag{2}$$

where C_{sat} is the satellite-predicted, C_{situ} is the *in situ* measured Chl-*a* and n is the number of match-ups.

In order to have a better understanding of the error, given that the units of the mentioned statistics are decades of log and are not easy to interpret, statistics on relative errors (RE) were derived empirically from the data. The distribution of the RE is approximately log-normal (not shown here) so the median of the RE distribution was used, given that it is more robust than the mean. The RE and the RMS (percentage) are defined as

$$\text{RE} = \frac{C_{sat}-C_{situ}}{C_{situ}} \tag{3}$$

and

$$\text{RMS} = \sqrt{\frac{1}{n}\sum(\text{RE})^2}\times 100\%. \tag{4}$$

Scatter plots of satellite versus *in situ* values for each algorithm were produced. A standard major axis (SMA) type II regression model was used to compute the slope and intercept of a linear equation that relates log-transformed *in situ* and satellite-derived Chl-*a* concentration. SMA techniques provide a better estimate of the line summarizing the relationship between two variables to that of ordinary linear regression, because the residual variance is minimized in both x and y dimensions, rather than in the y dimension only (Sokal and Rohlf 1995). The slope, intercept and the coefficient of determination (R^2) were obtained from the model II regression using (S)MATR software (version 1, Falster DS, Warton DI & Wright IJ: http://www.bio.mq.edu.au/ecology/SMATR/). The coefficient of determination indicates the overall degree of linear association between the log-transformed *in situ* and log-transformed satellite estimates, but it is not a measure of the algorithm performance. Thus, the slope (closer to 1), the intercept (closer to 0) and the mentioned statistics are used to evaluate the performance of the empirical algorithms.

4. Results and discussion

4.1 *Chl-a products evaluation*

The total number of *in situ* data points collected during the analysed cruises was 287 (figure 2(*a*)). Due to cloud cover and after applying the temporal window selection criteria (± 3 h), the match-ups were reduced to 39 for SeaWiFS and 24 for MODIS (figure 2(*b*)). These data cover a range of *in situ* Chl-*a* values from 0.2 to 6.1 mg m^{-3}. The reduced number of MODIS match-ups points compared to SeaWiFS is mainly due to the fact that the MODIS/Aqua system was launched in November 2002 and coincidental match-ups were available only for 2003 and 2004 cruises, thus less data were available for comparison.

Scatter plots of satellite versus *in situ* values for each product are shown in figures 3 and 4. The major correlation and statistics results of the algorithm evaluations are presented in table 3. Although on average the MODIS and SeaWiFS pigment algorithms underestimate the Chl-*a* concentrations, as shown by the

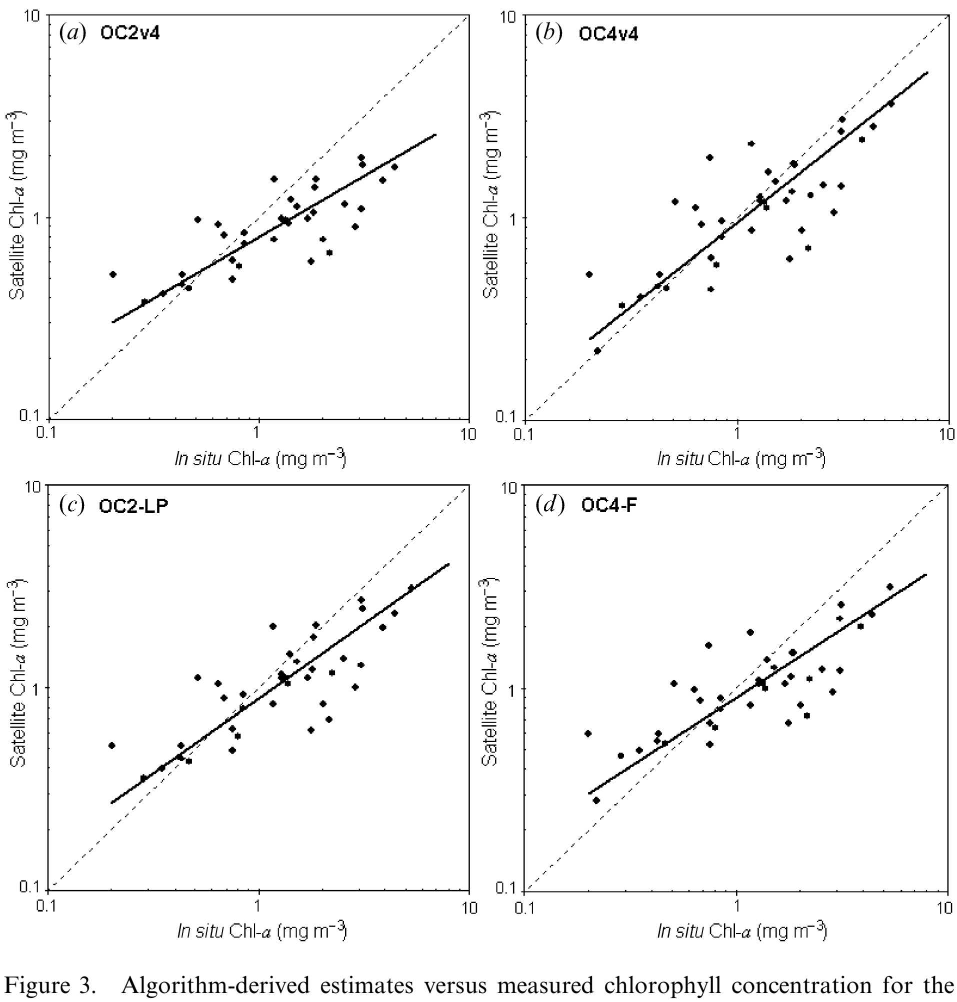

Figure 3. Algorithm-derived estimates versus measured chlorophyll concentration for the four SeaWiFS algorithms analysed: (*a*) OC2v4, (*b*) OC4v4, (*c*) OC2-LP and (*d*) OC4-F. The solid line is the linear relationship determined by model II least square regression. The dashed line represents a 1 : 1 relationship.

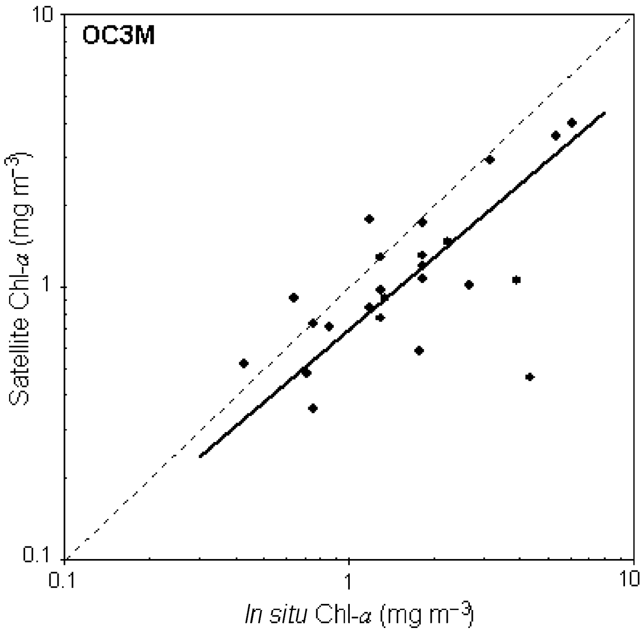

Figure 4. Algorithm-derived estimates versus measured Chl-*a* for the MODIS algorithm analysed (OC3M). The solid line is the linear relationship determined by model II least square regression. The dashed line represents a 1 : 1 relationship.

negative median relative error percent (table 3), a correlation with *in situ* Chl-*a* (within the range analysed here) can be observed in figures 3 and 4. In order to analyse this, the ratio of satellite to *in situ* measurements for the different algorithms and for two Chl-*a* ranges were calculated (table 4). It can be observed that for concentrations $<1.0\,\mathrm{mg\,m^{-3}}$, SeaWiFS's algorithms tend to overestimate Chl-*a* relative to *in situ* measurements by 20–40%, and at concentrations $>1.0\,\mathrm{mg\,m^{-3}}$, they tend to underestimate *in situ* values by 22–41%. Conversely, the MODIS algorithm shows an underestimation of *in situ* values within the whole concentration range here analysed by 7–32%. It should be noted that the reduced number of observations available for the low Chl-*a* values ($<1.0\,\mathrm{mg\,m^{-3}}$) for the MODIS algorithm ($n=8$) compared to SeaWiFS ($n=14$ and 16) could be responsible for the difference found. The plots of the relative error difference (RE) as a function of the *in situ* Chl-*a* range (figures 5 and 6) show that there is a general decrease in the

Table 3. Statistical results of the product evaluations. All linear correlations were statistically significant ($p<0.05$).

Algorithm	Slope	Intercept	R^2	n	RMS-log	BIAS-log	RMS (%)	RE (%)†
OC2v4	0.603	−0.098	0.585	38	0.264	−0.136	49.0	−27.4
OC4v4	0.826	−0.028	0.581	40	0.234	−0.040	54.7	−6.2
OC4-F	0.672	−0.040	0.550	40	0.247	−0.063	54.6	−18.3
OC2-LP	0.746	−0.056	0.580	38	0.235	−0.080	47.8	−15.1
OC3M	0.889	−0.162	0.403	24	0.303	−0.184	41.8	−32.4

†Median percent relative difference

Table 4. Ratio (mean ± standard deviation) of satellite-derived to *in situ* Chl-*a* values.

Algorithm	$<1\,mg\,m^{-3}$	$>1\,mg\,m^{-3}$
OC2v4	1.2 ± 0.48 ($n = 14$)	0.59 ± 0.23 ($n = 24$)
OC4v4	1.34 ± 0.62 ($n = 16$)	0.78 ± 0.34 ($n = 24$)
OC4-F	1.4 ± 0.56 ($n = 16$)	0.67 ± 0.26 ($n = 24$)
OC2-LP	1.24 ± 0.52 ($n = 14$)	0.72 ± 0.3 ($n = 24$)
OC3M	0.93 ± 0.32 ($n = 6$)	0.68 ± 0.3 ($n = 18$)

algorithm performance for concentrations $<1.0\,mg\,m^{-3}$. Moreover, the change of sign in the RE around $1.0\,mg\,m^{-3}$ can be clearly observed in the SeaWiFS algorithms, in agreement with the previously observed bias (figure 5).

The analysis of the statistical parameters (table 3) shows that a significant linear correlation between *in situ* and satellite-derived Chl-*a* for the five algorithms analysed was found. The correlation coefficient of the estimated versus the *in situ*

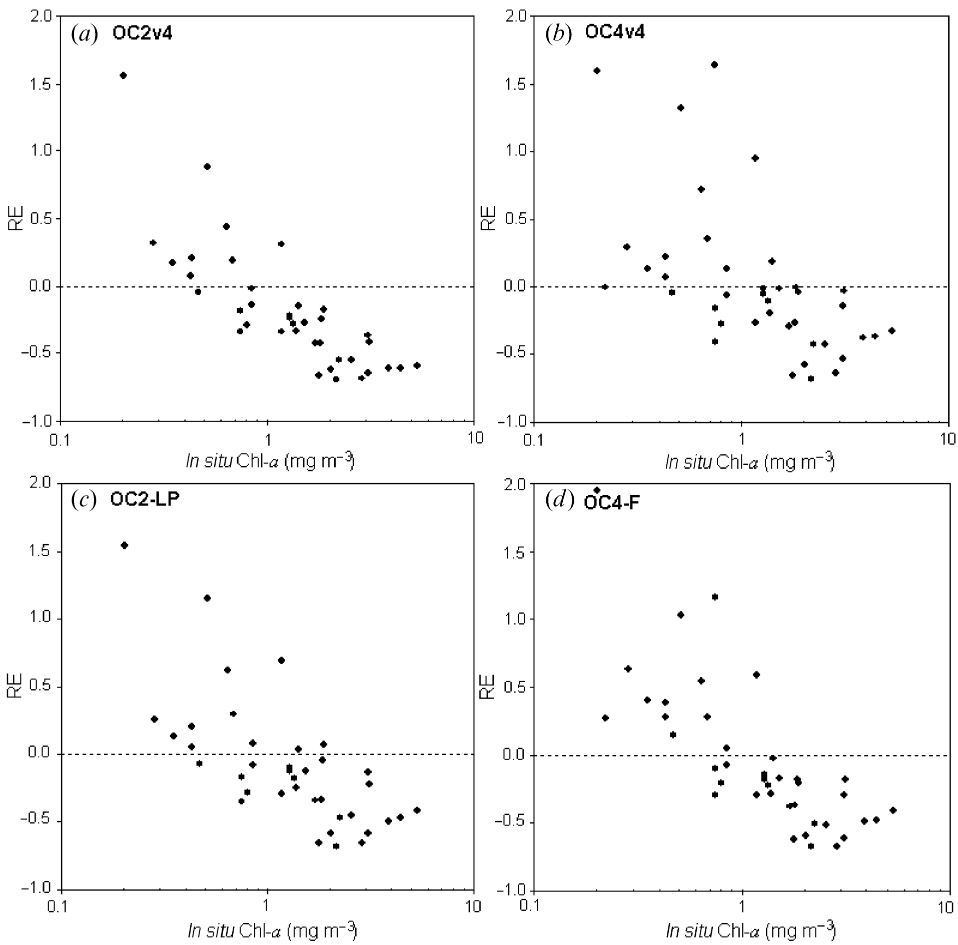

Figure 5. Relative errors in algorithm-derived estimates versus measured chlorophyll concentration for the four SeaWiFS algorithms analysed: (*a*) OC2v4, (*b*) OC4v4, (*c*) OC2-LP and (*d*) OC4-F.

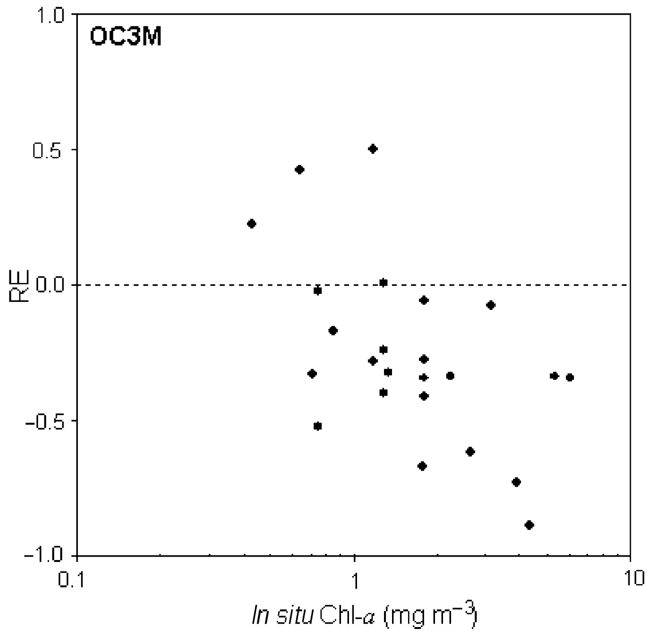

Figure 6. Relative errors in algorithm-derived estimates versus measured chlorophyll concentration for the MODIS algorithm analysed (OC3M).

Chl-*a* was very similar for all SeaWiFS algorithms (R^2~0.5 and $p < 0.05$), while the MODIS OC3M algorithm showed lower correlation ($R^2 = 0.403$ and $p < 0.05$). Even though OC3M showed the highest slope (0.889) and lowest RMS (41.8%), it showed the highest errors in log space and highest negative percent relative error (−32.4%). Again, the reduced number of MODIS match-ups could be influencing the algorithm's performance compared to the SeaWiFS algorithms. Among the SeaWiFS algorithms, OC2v4 showed the lowest slope (0.603), the highest negative intercept, log-errors, and the highest negative percent relative error (−27.4%), but comparatively lower RMS. The two regional algorithms, OC2-LP and OC4-F, performed slightly better than OC2v4, i.e. higher slopes (0.746 and 0.672), lower RMS-log, BIAS-log and lower, but still high, negative RE (−15.1% and −18.3%). On the other hand, the OC4v4 NASA operational algorithm exhibited the best statistical performance between the five tested algorithms, i.e. the slope is closer to 1 (0.826), the intercept closer to 0 (−0.028), lower log errors and lower RE (−6.2%). Even though the two regional algorithms were developed using bio-optical data from regions close to the study region, they did not clearly improve the global algorithm estimates. This can be due to the particular biophysical characteristics of the Patagonian Continental Shelf, which differ from the regions where *in situ* data were taken to develop the regional algorithms, i.e. South Atlantic gyre, southern Brazilian shelf and the La Plata River runoff region. Actually, the PCS is included within the Southwest Atlantic Continental Shelf (FKLD) province, according to Longhurst (1998), while the other regions are included in several different biomes and provinces with different characteristics, such as the Brazil Current (BRAZ), South Atlantic Tropical Gyre (SATL), South Subtropical Convergence (SSTC) and Subantarctic (SANT).

Differences between estimated and *in situ* Chl-*a* measurements can a rise either from failures in atmospheric correction procedures or from peculiar bio-optical characteristics of the PCS. Even though the NIR correction, introduced in the fourth reprocessing, accounts for water-leaving radiance in the NIR bands under conditions for which the black-pixel assumption is not valid (Patt *et al.* 2003), this correction scheme may not be entirely applicable for continental shelf waters, such as the PCS, as was shown in the comparison of SeaWiFS-derived normalized water-leaving values from the third and fourth reprocessing in a northeast portion of the US coast (Patt *et al.* 2003). Despite the improvements found, the fourth reprocessing still produced relatively high negative water-leaving values (meanly in the blue bands) in a large portion of the continental shelf area analysed, evidencing the need for improving atmospheric correction schemes, particularly in the near-shore areas. The presence of absorbing aerosols may also affect the atmospheric correction procedure since the aerosol models currently used are all non- or weakly absorbing (Gordon and Wang 1994); thus, their presence results in incorrect aerosol model selection influencing the satellite radiance retrievals, more significantly in the blue portion of the spectrum. Given that the satellite-derived product (Chl-*a*) analysed here was obtained by applying the algorithms to remotely sensed data and not to bio-optical measurements, as data on the water-leaving radiance was not available, it was not possible to evaluate or quantify the possible error induced by the atmospheric correction term. It should be noted that dust emission events from the Patagonian desert to the south Atlantic Ocean have been reported before using either surface measurements (Gaiero *et al.* 2003) or a combined approach of different satellite detectors and aerosol transport models (Gassó and Stein 2007). Surface studies showed that dust emissions follow a seasonal pattern, with highest dust activity in summer, although winter and autumn events have also been reported (Gaiero *et al.* 2003). The knowledge of dust activity in this area is mainly limited to modelling studies; more observational data are required in order to identify the major sources of dust, its long range transport, as well as the frequency of dust events. For our match-up data, the aerosol optical thickness at 865 nm, which is proportional to aerosol particle concentration from the ocean surface to the top of the atmosphere, varied over a fairly broad range from about 0.002 to 0.18. These low values ($\leqslant 0.2$) evidence clear atmosphere conditions (Kwiatkowska 2003), and therefore no evidence of the presence of a dust plume was found during the sampling dates. The presence of optically active components other than Chl-*a*, such as coloured dissolved organic matter (CDOM) or sediments may cause the blue to green reflectance ratio algorithms to return biased values. The composition of phytoplankton species present in the water (i.e. its shape, size and pigmentation) can also modify the optical characteristics of the water, causing a variation in the water-leaving radiance ratio independently of changes in the concentration of Chl-*a*, thus retrieving erroneous Chl-*a* values when empirical algorithms are used. An additional source of error may be the uncertainty in the *in situ* measurements. Spectrophotometric techniques applied in natural phytoplankton assemblages are known to have inadequate sensitivity, mainly at low chlorophyll concentrations (Jeffrey and Welschmeyer 1997). However, the Chl-*a* concentration found in the present comparison ranged between 0.2 and 6 mg m^{-3}, within which the method's sensitivity can be considered adequate. Furthermore, the determination of Chl-*a* by the spectrophotometric-acidification method may be biased by the presence of chlorophyll-*b* in the phytoplankton population (present in chlorophytes and prasinophytes), thus overestimating phaeopigments and finally underestimating Chl-*a* concentration. It is worth mentioning that uncertainties may also arise due to the fact that *in situ* samples were taken at the fixed depth of 9 m and, provided that information on the vertical biomass distribution is not available, the compared *in situ* measurement may not always be a good representation of the Chl-*a* observed by the satellite sensor. The information obtained by means of remote sensing is the pigment concentration within the penetration depth (z_{90}), defined by Gordon and McCluney (1975) as the layer thickness from which 90% of the total radiance originates. They showed that, for a homogeneous ocean, the penetration depth can be approximated with the inverse of the diffuse attenuation coefficient ($z_{90} \approx K^{-1}$). Nevertheless, if vertical distribution of the chlorophyll concentration is homogeneous, the Chl-*a* measured at 9 m depth could be comparable to the remote sensed values independently of the location of the penetration depth. On the other hand, a significant error could be introduced, reducing the algorithm performance, if a chlorophyll maximum or optically active substances were present above the sample depth and within the layer 'seen' by the remote sensor. In these cases, the optical properties of the water column influencing the remote sensing observations would be different to the optical properties of the water at the sampled depth. Consequently, more details on the vertical structure of the Chl-*a* are necessary to calculate the weighted mean pigment concentration within the surface layer, following Gordon and Clark (1980), in order to estimate the *in situ* chlorophyll concentration that is observed by the satellite. This calculation was not feasible in the present study given the lack information of the vertical structure of the water column.

The FKLD province, in which the PCS is included, is enclosed in the coastal boundary biome, where algal blooms are, in general, induced by shelf-break and coastal fronts and river discharges (Longhurst 1998). Several tidal fronts and the shelf-break front, coincident with the external shelf border (approximately along the 200 m isobath) have been previously described (Bava *et al.* 2002, Acha *et al.* 2004 and references therein), both of which are distinct features of the PCS. Furthermore, their association with high chlorophyll values has already been mentioned (Acha *et al.* 2004, Rivas 2006, Romero *et al.* 2006). Moreover, the PCS is also affected by the freshwater discharge from rivers along the Patagonian coast (the Colorado, Negro, Chubut, Deseado, San Julián, Chico, Santa Cruz, Coig and Gallegos rivers) and by the inflow of diluted waters from the Magellan Strait (figure 1) that may influence the optical properties of the coastal waters. Given the peculiar characteristic of the PCS, a more regional analysis within the PCS was performed in order to study the performance of the empirical algorithms and to identify the potential sources of discrepancy.

4.2 *Regional analysis*

The regional analysis was performed using the OC4v4 algorithm for SeaWiFS as it showed better statistical performance than the other SeaWiFS algorithms. For MODIS, the OC3M was used as it is the current default algorithm and it is the MODIS version of the SeaWiFS OC4 algorithm (uses similar bands and is based on the same global dataset). However, OC3M estimates proved to be less accurate than OC4v4. This could be related to the small number of match-ups available for OC3M analysis ($n = 24$) compared to OC4v4 ($n = 40$). Furthermore, differences in calibration and in the atmospheric correction applied may partially account for the difference in algorithm performance.

In order to make use of the Chl-*a* estimates of both sensors together, a comparison between them and *in situ* data was performed. The relative errors of the OC4v4 and OC3M with respect to the *in situ* data, using equation (3), for the coincident match-ups were calculated. Furthermore, the relative percent error between the satellite-derived Chl-*a* products, i.e. using OC3M (C_{OC3M}) and OC4v4 (C_{OC4v4}), relative to their average (RE_s) was calculated using the following equation:

$$RE_S = \frac{C_{OC3M} - C_{OC4v4}}{(C_{OC3M} + C_{OC4v4})/2} \times 100\%. \quad (5)$$

The relative percent error between sensors (RE_s) ranged from −40% to 7%, with a median of −4.6%, and was much smaller than the error between the satellite-derived estimates and *in situ* data (RE), which ranged from −65% to 95% for OC4v4 and from −73% to 50% for OC3M, with medians of −21.1% and −30.3%, respectively (see figure 7). This result shows that the error between the two sensor estimates is much smaller than between the estimates and the *in situ* data, allowing us to use both sensors together in the regional analysis.

With the intention of analysing the performance of the empirical algorithms regionally and the possible causes of the algorithm failure, the more stringent match-up dataset (used to compare the algorithms) was sorted into five subsets (figure 8). One group was constituted by the stations located in the homogeneous side of the tidal fronts (TF) found in the PCS (hatched area in figure 8). The near-summer mean position of the tidal fronts has been determined by Bianchi *et al.*

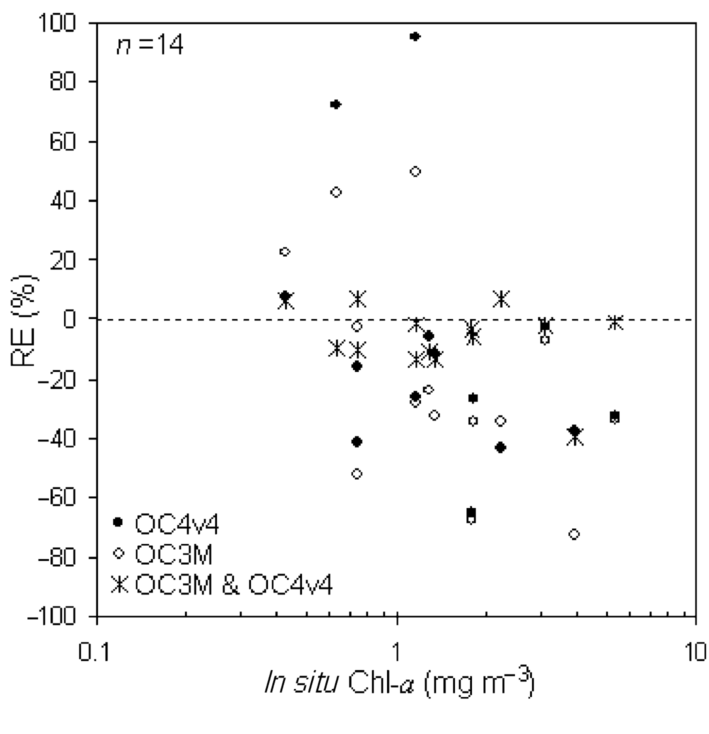

Figure 7. Relative percent error between satellite-derived estimates (OC4v4 and OC3M) and *in situ* data and between the sensor estimates and their average (OC3M and OC4v4) versus measured chlorophyll-*a* concentration. The number of coincident match-ups analysed is indicated (*n*).

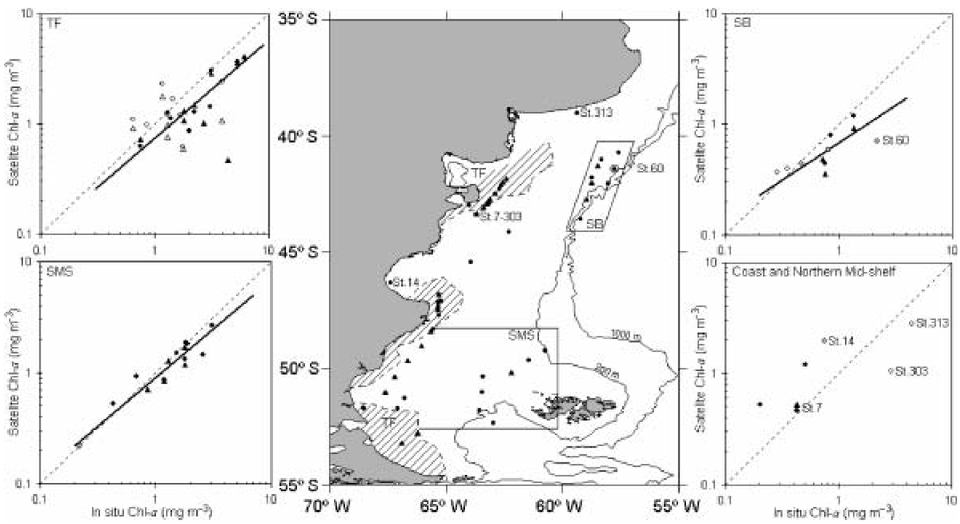

Figure 8. Location of the match-up stations and the subsets defined in the text (TF: homogeneous side of tidal fronts, SMS: southern mid-shelf, SB: shelf-break area and the coastal and central mid-shelf match-ups plotted together). Triangles correspond to MODIS and circles to SeaWiFS estimates. Black-filled symbols correspond to summer, open symbols to autumn and grey-filled symbols to winter cruises. The number of some stations mentioned in the text is included.

(2005) on the basis of the Simpson parameter that measures the magnitude of the vertical stratification of the water column (dashed line in figure 8 corresponds to the critical Simpson parameter $\Phi_c = 50\,\mathrm{J\,m^{-1}}$ used in Bianchi *et al.* (2005) to define the location of tidal fronts). Another group was formed by the stations located in the northern part of the shelf break, close to the shelf-break front (see figure 1). The stations located in the southern mid-shelf, south of 47° S approximately and west of the Malvinas (Falkland) Islands, were analysed together as a group, and finally three stations remained located in the central mid-shelf and two stations in very coastal waters (south of Buenos Aires Province and in San Jorge Gulf). The last two groups are plotted together on the same graph for convenience, but no regression or statistics were calculated due to the scarce number of data and the dissimilar oceanographic environments each of them belongs to. The plots and the statistics (figure 8 and table 5) clearly show spatial differences in the algorithm performances. The data analysed here were collected at different times of the year, i.e. summer, autumn and winter (see table 1), but a seasonal analysis was not performed since the number and spatial coverage of the seasonal subsets were not evenly distributed. However, the season that corresponds to each match-up is indicated in the plots in figure 8 and will be taken into account in the analysis.

The match-ups located in the homogeneous side of tidal fronts showed the lowest, though significant, correlation between *in situ* and satellite-derived Chl-*a* with $R^2 = 0.28$ ($p < 0.05$), and the highest scatter and negative bias, in both linear and log space (RMS = 45.9%, RE = −29.4% and RMS-log = 0.298, BIAS-log = −0.159). The presence of sediments, originated either from re-suspension of bottom sediments or river runoff, as well as particulate and dissolved detrital material of terrestrial origin, may partially explain the poor performance of the empirical algorithms in these regions. Even though no optical data are available to support

Table 5. Statistical results of the regional analysis. All linear correlations were statistically significant ($p<0.05$).

Region	Slope	Intercept	R^2	n	RMS-log	BIAS-log	RMS (%)	RE (%)†
TF	0.89	−0.129	0.276	31	0.298	−0.159	45.9	−29.4
SB	0.67	−0.171	0.561	11	0.212	−0.132	34.5	−27.5
SMS	0.88	−0.044	0.893	15	0.112	−0.055	22.5	−5.8

†Median percent relative error

this hypothesis, these areas probably belong to case 2 waters (either sediment-dominated or yellow substance dominated waters), where empirical case 1 water algorithms fail, generally overestimating Chl-*a*. Supporting this idea, the inclusive case 1 remote-sensing criterion developed by Lee and Hu (2006), applied here to seasonally averaged 4 km SeaWiFS GAC data for the period of study, showed that the non-case 1 waters spatial distribution clearly resembled the areas delineated by the critical Simpson parameter (figure 9). The global distribution shown in the work of Lee and Hu (2006), using 9 km SeaWiFS data, shows the whole PCS belonging to non-case 1 waters. However, analysing the higher resolution 4 km SeaWiFS images, more detailed information on the spatial distribution of the non-case 1 waters was obtained. Figure 9 shows the seasonal distribution of non-case 1 waters for summer, autumn and winter 2001, yet similar patterns were obtained in the seasonal maps for 2003 and 2004 (not shown here). Conversely, the underestimation at high Chl-*a* in this region, mainly in summer (black-filled symbols in figure 8), could be related to the presence of large-size diatoms that may influence the optical properties of the water in the homogeneous side of the tidal fronts. Carreto *et al.* (1986) found that chain-forming diatoms are abundant in similar areas off Valdés Peninsula and also in the tidal front located in the southern limit of San Jorge Gulf (Carreto *et al.* 2006). A decrease in the specific absorption coefficient of phytoplankton (i.e. the absorption coefficient of phytoplankton per unit of Chl-*a*) due to the particle effect (also known as the 'package effect') when large-size cells are present may lead to a

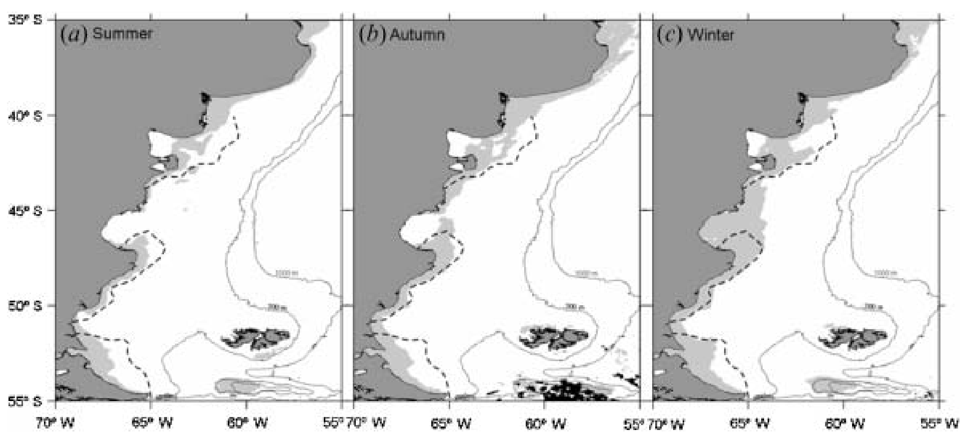

Figure 9. Local distribution of non-case 1 waters (light grey) for (*a*) summer, (*b*) autumn and (*c*) winter 2001, using Lee and Hu (2006) criterion for determining case 1 waters. Dashed line corresponds to the summer mean tidal front location defined by the critical Simpson parameter used in Bianchi *et al.* (2005). Pixels that have negative remote sensing reflectance in any band are shown in black.

significant underestimation in the retrieved Chl-*a* using empirical algorithms (Sathyendranath *et al.* 2001). This package or particle effect theoretically predicts the flattening of the absorption spectra (i.e. a decrease of the absorption efficiency) with increasing cell size and pigment concentrations (Duysens 1956, Sathyendranath *et al.* 1987).

The shelf-break area is a very dynamic region, where the subantarctic shelf waters meet the cooler and more saline waters of the Malvinas current producing a thermohaline front. The geographical location of the front may vary according to the dynamics of the Malvinas current, for which cyclical variations have been reported (Olson *et al.* 1988). In this area, the largest difference between *in situ* and satellite-derived values was found in one station sampled in winter (St. 60), located in a relatively high Chl-*a* patch observed in the satellite image, probably a phytoplankton bloom with measured chlorophyll concentration of 2.17 $mg\,m^{-3}$, but with a satellite estimate of 0.58 $mg\,m^{-3}$. Differences in the optical properties of the phytoplankton assemblage due to variation in the size structure of the phytoplankton population (particle effect) or in the pigment composition, may partially contribute to this significant difference between *in situ* and satellite-derived Chl-*a* values. The phytoplankton assemblage at this station was dominated by medium size (6–20 μm) organisms that account for 50% of the total cell number. Cryptophytes ($\sim 9.3 \times 10^4$ cells/litre), dinoflagellates ($\sim 3 \times 10^4$ cells/litre), prasinophytes ($\sim 1.4 \times 10^4$ cells/litre) and other unidentified flagellates were the main taxa contributing to this group. Moreover, the presence of the large-size diatom *Corethron pennatum*, which was observed at densities of about 6×10^4 cells/litre, was also prominent. In addition, the pigment composition (type and amount of auxiliary pigments relative to Chl-*a* present in the sample) that may result from the adaptation to the light and nutrient regimes, and an increase of intra-cellular Chl-*a*, resulting as an adaptation to low light levels (winter time and low latitude), can be hypothesized to be also responsible for the underestimation of the satellite-derived Chl-*a* value. Information on bio-optical properties (such as the phytoplankton absorption coefficient) and pigment composition would contribute very valuable information to test this hypothesis. The differences found for the summer stations between *in situ* and satellite-derived Chl-*a* could be due to differences between the optical properties at the sampled depth (9 m) and the properties influencing the remote sensed signal in a probable stratified water column.

Regarding the two coastal stations (St. 14 and 313, see figure 8), significant differences between them should be mentioned. The more southern coastal station (St. 14), located in San Jorge Gulf, was sampled in winter and presented low Chl-*a* (0.74 $mg\,m^{-3}$), that was overestimated by the OC4v4 algorithm (figure 8). During this season, the water column is well-mixed, with high amount of sediments due probably to re-suspension from the bottom in the shallow coastal zone. This is evidenced by high normalized water-leaving radiance values at 555 nm found all along the coast in the SeaWiFS images analysed for the 8 day period in coincidence with the cruise survey (not shown here) and by the spatial distribution of non-case 1 waters for winter (figure 9). Empirical algorithms break down in case 2 waters, probably due to failure in the black pixel assumption for the NIR bands caused by the presence of a high amount of sediment in the water column. The most conspicuous feature of the phytoplankton assemblage in this station was the presence of high concentration of medium-size ($\sim$10 μm) Gymnodinioid dinoflagellates reaching high densities (2.7×10^5 cells/litre). Moreover, small unidentified flagellates (<5 μm) were also present at high concentrations (2.8×10^5 cells/litre), whereas large-size (>20 μm) diatoms were poorly represented, accounting for less than 4% of the total cell number. Conversely, the northern coastal station located in the southern coast of Buenos Aires province (St. 313) was sampled in autumn (2004) and presented relatively high Chl-*a* (4.46 mg m^{-3}), which was underestimated by the satellite estimates (figure 8). We can speculate that at least part of the difference between *in situ* and satellite-derived values can be caused by the phytoplankton community structure, which was characterized by the presence of large-size (>20 μm) organisms, representing more than 70% of the total cell number. This assemblage was dominated by the chain-forming diatom *Bacteriastrum delicatulum*, which reached high densities ($\sim 2.5 \times 10^5$ cells/litre) and accounted for more than 50% of total cell abundance. Moreover, other chain-forming diatoms such as *Chaetoceros* spp., *Pseudo-nitzschia* spp. and *Hemiaulus* sp., and prominent solitary diatoms and dinoflagellates such as *Meuniera membranacea* and *Dinophysis caudata*, respectively, were also represented. As mentioned previously, the dominance of relatively large-size cells in the phytoplankton assemblage may be evidencing the flattening of the specific absorption spectra (particle or package effect), leading to a significant underestimation by the empirical satellite-retrieved Chl-*a* values (Sathyendranath *et al.* 2001). This effect was noted by Lutz *et al.* (2006) in the 'EPEA' coastal station, located relatively close to the station analysed here, where a bloom of a large-size diatom (*Coscinodiscus wailesii*) with a very low specific absorption coefficient was detected.

An interesting case of two samples collected in 2003 that almost coincided spatially, but one sampled in summer (St. 7) and the other in autumn (St. 303), deserves a more detailed analysis. The satellite algorithms performed differently in each case (see plot in figure 8). In St. 7 (summer) the satellite-derived values were in good agreement with the measured values, whereas in St. 303 (autumn) the algorithm clearly underestimated *in situ* Chl-*a*. Both stations are located south of Valdés Peninsula, on the stratified side of the tidal front (figure 8) and neither the influence of land was observed, nor any of the processing flags regarding atmospheric correction failure in the output product was set. In order to analyse the performance of the atmospheric correction procedure, coincidental *in situ* water-leaving radiance measurements are necessary. However, information on the phytoplankton composition helped to understand the seasonal difference found in the algorithm retrievals. Chl-*a* concentration at St. 7 and St. 303 were 0.5 and 3.65 mg m^{-3}, respectively. In both stations, unidentified tiny phytoflagellates (<5μm) numerically dominated the phytoplankton assemblages, accounting for 87% (St. 7) and 69% (St. 303) of the total cell numbers. However, the contribution of <5 μm cells to total Chl-*a* was 73% in St. 7 and only 32% in St. 303, in which a high density ($\sim 3.5 \times 10^4$ cells/litre) of the dinoflagellate *Prorocentrum micans* was observed. Summarizing, the presence of large-size species in St. 303 (where >10 μm cells contributed with ~70% to the total Chl-*a*) may probably be influencing the optical characteristics of the phytoplankton, even though the small fraction (<5 μm) numerically dominated the phytoplankton assemblage. Again, this could be evidencing the so-called pigment package effect, but this hypothesis could not be verified.

The performance of the algorithms was clearly better when the match-up data points used were located in the southern mid-shelf. The correlation coefficient shows a good linear relationship ($R^2 = 0.89$), the slope is closer to 1 (0.88) and the intercept closer to 0 (−0.044). The scatter (RMS = 22.5% and RMS-log = 0.112) and bias (RE = −5.8% and BIAS-log = −0.055) are much lower than for the other areas and for the whole PCS dataset, showing a better agreement between *in situ* and satellite-derived values. One possible explanation could be that this region is less influenced by land input, such as river discharge or re-suspension of bottom sediments, thus showing a general tendency towards better agreement with *in situ* data over the other subsets analysed previously. Krepper and Rivas (1979) found that the stratification of the water column in the austral region of the shelf is mainly controlled by temperature. In summer, stratification can be found up to 51° S and is almost negligible south of that latitude, where most of the stations within this region were sampled. If this were the case, it suggests that the good agreement found between the *in situ* and the satellite estimates could be related to the homogeneity of the water column and that the Chl-*a* measured at 9 m depth would be thus a good representation of the Chl-*a* observed by the satellite sensor, even if the samples were taken in summer. In order to corroborate this, information of the vertical structure of the water column would be necessary. It should be noted that since most of the match-ups were sampled in summer and only one station was sampled in autumn, more measurements at different times of the year are needed if a seasonal analysis of the empirical algorithms performance is desired.

5. Summary and conclusions

In this paper, uncertainties in the retrieval of satellite-derived surface Chl-*a* concentration have been evaluated in the Patagonian Continental Shelf for the first time. Regional and global ocean colour products have been compared to *in situ* Chl-*a* measurement collected on five cruises between 2000 and 2004. A systematic error was found in the satellite-derived Chl-*a* for all SeaWiFS algorithms analysed, showing a general overestimation at low Chl-*a* ($<1\ \mathrm{mg\,m^{-3}}$) and an underestimation at high Chl-*a* ($>1\ \mathrm{mg\,m^{-3}}$). On the other hand, the MODIS algorithm showed a general underestimation over the whole range analysed. The results of the analysis showed that the OC4v4 standard algorithm performs better than the global OC2v4 and the two existing regional algorithms (OC4-F and OC2-LP), at least during the time interval of our dataset (2000–2004). It is worth noting that the accuracy found in the present study of the satellite-derived Chl-*a* using OC4v4 algorithm does not differ much from the accuracy of the algorithm from which it is derived, i.e. RMSE in log units 0.222 (O'Reilly *et al.* 2000).

The difference found between MODIS and SeaWiFS Chl-*a* data was smaller than between satellite and *in situ* data. The relative differences between the two datasets are generally $<\pm 15\%$ for the coincidental match-ups. The regional analysis, using the Chl-*a* product of both sensors together, showed that there was a substantial difference in the performance of the SeaWiFS and MODIS algorithms regarding the location of the sampled sites. For the first time, non-case 1 and probable case 2 waters were identified in the PCS. These areas are mainly influenced by tidal mixing and river runoff. Information on the taxonomic composition and cell abundance, in coincidence with match-ups and similar data from previous studies in the region, provided useful information that helped understanding and partially explained the contribution of the phytoplankton composition to the differences found between *in situ* and satellite-derived values. This shows the importance of using not only bio-optical, but also taxonomic data, to evaluate their impact on the retrieval of remotely-sensed Chl-*a*. For a seasonal and more comprehensive analysis, a larger dataset of bio-optical *in situ* measurements is clearly necessary.

Acknowledgements

A.I. Dogliotti would like to thank R. Frouin and G. Giribet for useful conversations and constructive comments on the manuscript, S. Bélanger for helpful suggestions on an earlier draft and the IOCCG and POGO for economical support in training programmes. Anonymous reviewers are acknowledged for their helpful comments. This work was supported by CONICET, Agencia Nacional de Promoción Científica y Tecnológica through grants PICTO 6524/1108/03-ANPCyT 01-11563 to I.R.S. and PICT03-15221 to D.A.G. The Global Environmental Facility (GEF) grant 28385 to D.A.G. and CONICET fellowships to A.I. Dogliotti and G.O. Almandoz. We thank the NASA SeaWiFS Project and the NASA/GSFC/DAAC for the production and distribution of SeaWiFS data, respectively. Field work was conducted within the framework of a cooperative research program (ARGAU, Programme de coopération avec la ARGentine pour l'étude de l'océan Atlantique AUstral) between the Instituto Antártico Argentino, the Laboratoire de Biogéochimie et Chimie Marines at the Université Pierre et Marie Curie in Paris (France), and the Servicio de Hidrografía Naval (Argentina) from 2002 to 2004. We wish to thank all the persons participating in sample collection, especially to A. Ulrich for Chl-*a* determinations. Our thanks also to the crew members of the *Almirante Irizar*.

References

ACHA, E.M., MIANZAN, H.W., GUERRERO, R.A., FAVERO, M. and BAVA, J., 2004, Marine fronts at the continental shelves of austral South America, physical and ecological processes. *Journal of Marine Systems*, **44**, pp. 83–105.

ANDERSEN, P. and THRONDSEN, J., 2003, Estimating cell number. In *Manual on Harmful Marine Microalgae*, Monographs on Oceanographic Methodology, **11**, G.M. Hallegraeff, D.M. Anderson and A.D. Cembella (Eds), pp. 99–129 (Paris: UNESCO).

ARMSTRONG, R.A., GILBES, F., GUERRERO, R., LASTA, C., BENAVIDES, H.R. and MIANZAN, H., 2004, Validation of SeaWiFS-derived chlorophyll for the Rio de la Plata Estuary and adjacent waters. *International Journal of Remote Sensing*, **25**, pp. 1501–1505.

BAILEY, S. and WERDELL, P., 2006, A multi-sensor approach for the on-orbit validation of ocean color satellite data products. *Remote Sensing of Environment*, **102**, pp. 12–23.

BAILEY, S.W., MCCLAIN, C.R., WERDELL, P.J. and SCHIEBER, B.D., 2000, Normalized water-leaving radiance and chlorophyll-a match-up analyses. In *SeaWiFS Postlaunch Technical Report Series*, **10**, *SeaWiFS Postlaunch Calibration and Validation Analyses*, Part 2. NASA Tech. Memo. 2000-206892, **10**, S.B. Hooker and E.R. Firestone (Eds), pp. 45–52 (Greenbelt, MD: NASA/Goddard Space Flight Center).

BAITH, K., LINDSAY, R., FU, G. and MCCLAIN, C.R., 2001, SeaDAS, a data analysis system for ocean-color satellite sensors. *EOS Transactions AGU*, **82**, p. 202.

BALESTRINI, C.F., POISSON, A.R., FERREYRA, G.A., FERRARIO, M.E., SCHAUER, B., SCHLOSS, I.R., MOLINA, D.A., SALA, H., BIANCHI, A.A., RUIZ-PINO, D., PIOLA, A.R. and SARACENO, M., 2000, Project 'ARGAU'. *Preliminary data-report I/B A.R.A. Almte. Irízar, Cruise ARGAU ZERO*, Report 529 (Buenos Aires, Argentina: Instituto Antártico Argentino).

BARRÉ, N., PROVOST, C. and SARACENO, M., 2006, Spatial and temporal scales of the Brazil–Malvinas Current confluence documented by simultaneous MODIS Aqua 1.1-km resolution SST and color images. *Advances in Space Research*, **37**, pp. 770–786.

BAVA, J., GAGLIARDINI, D.A., DOGLIOTTI, A.I. and LASTA, C.A., 2002, Annual distribution and variability of remotely sensed sea surface temperature fronts in the Southwestern Atlantic Ocean. In *29th International Symposium on Remote Sensing of the Environment, International Society for Remote Sensing of the Environment*, 8–12 April 2002, Buenos Aires, Argentina.

BEHRENFELD, M.J. and FALKOWSKI, P.G., 1997, Photosynthetic rates derived from satellite-based chlorophyll concentration. *Limnology and Oceanography*, **42**, pp. 1–20.

BIANCHI, A.A., BIANUCCI, L., PIOLA, A.R., RUIZ PINO, D., SCHLOSS, I., POISSON, A. and BALESTRINI, C.F., 2005, Vertical stratification and air–sea CO_2 fluxes in the Patagonian shelf. *Journal of Geophysical Research*, **110**, C07003.

CAMPBELL, J.W., 1995, The lognormal distribution as a model for bio-optical variability in the sea. *Journal of Geophysical Research*, **100**, pp. 13237–13254.

CARRETO, J.I., BENAVIDES, H.R., NEGRI, R.M. and GLORIOSO, P.D., 1986, Toxic red-tide in the Argentine Sea. Phytoplancton distribution and survival of the toxic dinoflagelate Gonyaulax excavata in a frontal area. *Journal of Plankton Research*, **8**, pp. 15–28.

CARRETO, J.I., CARIGNAN, M.O., MONTOYA, N.G. and CUCCHI COLLEONI, D.A., 2006, Dinámica del fitoplancton en el sistema frontal del golfo San Jorge. In *VI Jornadas Nacionales de Ciencias del Mar y XIV Coloquio de Oceanografía*, 4–8 December 2006, Puerto Madryn, Argentina.

DARECKI, M., KACZMAREK, S. and OLSZEWSKI, J., 2005, SeaWiFS ocean colour chlorophyll algorithms for the southern Baltic Sea. *International Journal of Remote Sensing*, **26**, pp. 247–260.

DING, K. and GORDON, H.R., 1994, Atmospheric correction of ocean color sensors: effects of the Earth curvature. *Applied Optics*, **33**, pp. 7096–7106.

DUYSENS, L.M.N., 1956, The flattening effect of the absorption spectra of suspensions as compared to that of solutions. *Biochimica et Biophysica Acta*, **19**, pp. 1–12.

FORBES, M.C. and GARRAFFO, Z.D., 1988, A note on the mean seasonal transport on the Argentinean shelf. *Journal of Geophysical Research*, **93**, pp. 2311–2319.

GAIERO, D.M., PROBST, J.L., DEPETRIS, P.J. and LELEYTER, L., 2003, Iron and other transition metals in Patagonian riverborne and windborne materials: geochemical control and transport to the southern South Atlantic Ocean. *Geochimica et Cosmochimica Acta*, **67**, pp. 3603–3623.

GARCIA, C.A.E., GARCIA, T.V.M. and MCCLAIN, C., 2005, Evaluation of SeaWiFS chlorophyll algorithms in the Southwestern Atlantic and Southern Oceans. *Remote Sensing of Environment*, **95**, pp. 125–137.

GARCIA, C.A.E., SARMA, Y.V.B., MATA, M.M. and GARCIA, V.M.T., 2004, Chlorophyll variability and eddies in the Brazil–Malvinas Confluence region. *Deep Sea Research Part II*, **51**, pp. 159–172.

GARCIA, V.M.T., SIGNORINI, S., GARCIA, C.A.E. and MCCLAIN, C., 2006, Empirical and semi-analytical chlorophyll algorithms in the southwestern Atlantic coastal region (25–40° S and 60–45° W). *International Journal of Remote Sensing*, **27**, pp. 1539–1562.

GASSÓ, S. and STEIN, A.F., 2007, Does dust from Patagonia reach the sub-Antarctic Atlantic Ocean? *Geophysical Research Letters*, **34**, L01801.

GLORIOSO, P.D. and FLATHER, R.A., 1997, The Patagonian Shelf tides. *Progress in Oceanography*, **40**, pp. 263–283.

GONZALEZ-SILVERA, A., SANTAMARIA-dEL-ANGEL, E., GARCIA, V.M.T., GARCIA, C.A.E., MILLÁN-NUÑEZ, R. and MÜLLER-KARGER, F., 2004, Biogeographical regions of the tropical and subtropical Atlantic Ocean off South America: classification based on pigment (CZCS) and chlorophyll-a (SeaWiFS) variability. *Continental Shelf Research*, **24**, pp. 983–1000.

GORDON, H.R. and CLARK, D.K., 1980, GRemote sensing optical properties of a stratified ocean: an improved interpretation. *Applied Optics*, **19**, pp. 3428–3430.

GORDON, H.R. and MCCLUNEY, W.R., 1975, Estimation of the depth of sunlight penetration in the sea for remote sening. *Applied Optics*, **14**, pp. 413–416.

GORDON, H.R. and WANG, M., 1994, Retrieval of water-leaving radiance and aerosol optical thickness over the oceans with SeaWiFS: a preliminary algorithm. *Applied Optics*, **33**, pp. 443–452.

HOOKER, S.B. and MCCLAIN, C.R., 2000, The calibration and validation of SeaWiFS data. *Progress in Oceanography*, **45**, pp. 427–465.

JEFFREY, S.W. and WELSCHMEYER, N.A., 1997, Spectrophotometric and fluorometric equations in common use in oceanography. In *Phytoplankton Pigments in Oceanography: Guidelines to Modern Methods*, S.W. Jeffrey, R.F. Mantoura and S.W. Wright (Eds), pp. 597–615 (Paris: SCOR-UNESCO).

KREPPER, C.M. and RIVAS, A.L., 1979, Análisis de las características oceanográficas de la zona austral de la Plataforma Continental Argentina y aguas adyacentes. *Acta Oceanographica Argentina*, **2**, pp. 55–82.

KWIATKOWSKA, E., 2003, Comparisons of daily global ocean color data sets: MODIS Terra/Aqua and SeaWiFS. In *MODIS Validation, Data Merger and Other Activities Accomplished by SIMBIOS Project: 2002–2003*, *TM–2003*, G.S. Fargion and C.R. McClain (Eds), pp. 2–18, SIMBIOS Project (Greenbelt, MD: NASA Goddard Space Flight Center).

LEE, Z.P. and HU, C., 2006, Global distribution of case-1 waters: an analysis from SeaWiFS measurements. *Remote Sensing of Environment*, **101**, pp. 270–276.

LONGHURST, A., 1998, *Ecological Geography of the Sea* (London: Academic Press).

LONGHURST, A., SATHYENDRANATH, S., PLATT, T. and CAVERHILL, C., 1995, An estimate of global primary production in the ocean from satellite radiometer data. *Journal of Plankton Research*, **17**, pp. 1245–1271.

LUTZ, V., SUBRAMANIAM, A., NEGRI, R., SILVA, R. and CARRETO, J.I., 2006, Annual variations in bio-optical properties at the 'Estación Permanente de Estudios Ambientales (EPEA)' coastal station, Argentina. *Continental Shelf Research*, **26**, pp. 1093–1112.

MOREL, A. and ANTOINE, D., 2007, *ATBD 2.9: Pigment index retrieval in case 1 waters*, ESA, Noordwijk, The Netherlands, ESA Doc. no. PO-TN-MEL-GS-0005. Available online at: http://envisat.esa.int/instruments/meris/pdf/atbd_2_09.pdf (accessed 17 January 2007).

MOREL, A. and PRIEUR, L., 1977, Analysis of variations in ocean color. *Limnology and Oceanography*, **22**, pp. 709–722.

OLSON, D.B., PODESTÁ, G.P., EVANS, R.H. and BROWN, O.B., 1988, Temporal variations in the separation of Brazil and Malvinas Currents. *Deep Sea Research*, **35**, pp. 1971–1990.

O'REILLY, J.E., MARITORENA, S., MITCHELL, B.G., SIEGEL, D.A., CARDER, K.L., GARVER, S.A., KAHRU, M. and MCCLAIN, C.R., 1998, Ocean color chlorophyll algorithms for SeaWiFS. *Journal of Geophysical Research*, **103**, pp. 24937–24953.

O'REILLY, J.E., MARITORENA, S., SIEGEL, D.A., O'BRIEN, M.C., TOOLE, D., MITCHELL, B.G., KAHRU, M., CHAVEZ, F.P., STRUTTON, P., COTA, G.F., HOOKER, S.B., MCCLAIN, C.R., CARDER, K.L., MÜLLER-KARGER, F., HARDING, L., MAGNUSON, A., PHYNNEY, D., MOORE, G.F., AIKEN, J., ARRIGO, K., LETELIER, R. and CULVER, M., 2000, Ocean color chlorophyll a algorithms for SeaWiFS, OC2, and OC4: version 4. In *SeaWiFS Postlaunch Calibration and Validation Analyses*, Part 3, NASA Tech. Memo. 2000-206892, **11**, S.B. Hooker and E.R. Firestone (Eds), pp. 9–23 (Greenbelt, MD: NASA Goddard Space Flight Center).

PATT, F.S., BARNES, R.A., EPLEE, R.E., FRANZ, B.A., ROBINSON, W.D., FELDMAN, G.C., BAILEY, S.W., GALES, J., WERDELL, P.J., WANG, M., FROUIN, R., STUMPF, R.P., ARNONE, R.A., GOULD, R.W. and MARTINOLICH, P.M., 2003, Algorithm updates for the fourth SeaWiFS data reprocessing. In *SeaWiFS Postlaunch Technical Report Series*, **22**, *Algorithms Updates for the Fourth SeaWiFS Data Reprocessing*. NASA Tech. Memo. 2003-206892, **22**, S.B. Hooker and E.R. Firestone (Eds) (Greenbelt, MD: NASA/Goddard Space Flight Center).

PIOLA, A.R. and RIVAS, A.L., 1997, Corrientes en la Plataforma Continental. In *El Mar Argentino y sus Recursos Pesqueros*, **1**, E. Boschi (Ed.), Inst. Nac. Invest. y Desarrollo Pesquero, Mar del Plata, Argentina), pp. 119–132.

PODESTÁ, G.P., 1997, Utilización de datos satelitarios en investigaciones oceanográficas y pesqueras en el océano Atlántico Sudoccidental. In *El Mar Argentino y sus Recursos*

Pesqueros, **1**, E. Boschi (Ed.), Inst. Nac. Invest. y Desarrollo Pesquero, Mar del Plata, Argentina), pp. 195–222.

RIVAS, A.L., 2006, Quantitative estimation of the influence of surface thermal fronts over chlorophyll concentration at the Patagonian shelf. *Journal of Marine Systems*, **63**, pp. 183–190.

RIVAS, A.L., DOGLIOTTI, A.I. and GAGLIARDINI, D.A., 2006, Satellite-measured surface chlorophyll variability in the Patagonian shelf. *Continental Shelf Research*, **26**, pp. 703–720.

ROMERO, S.I., PIOLA, A.R., CHARO, M. and GARCIA, C.A.E., 2006, Cholorophyll-*a* variability off Patagonia based on SeaWiFS data. *Journal of Geophysical Research*, **111**, C05021.

SARACENO, M., PROVOST, C. and LEBBAH, M., 2006, Biophysical regions identification using an artificial neuronal network: a case study in the South Western Atlantic. *Advances in Space Research*, **37**, pp. 793–805.

SARACENO, M., PROVOST, C. and PIOLA, A.R., 2005, On the relationship between satellite retrieved surface temperature fronts and chlorophyll-a in the Western South Atlantic. *Journal of Geophysical Research*, **110**, C11016.

SATHYENDRANATH, S., LAZZARA, L. and PRIEUR, L., 1987, Variations in the spectral values of specific absorption of phytoplankton. *Limnology and Oceanography*, **32**, pp. 403–415.

SATHYENDRANATH, S., COTA, G., STUART, V., MAASS, H. and PLATT, T., 2001, Remote sensing of phytoplankton pigments: a comparison of empirical and theoretical approaches. *International Journal of Remote Sensensing*, **22**, pp. 249–273.

SATHYENDRANATH, S., BUKATA, R.P., ARNONE, R., DOWELL, M.D., DAVIS, C.O., BABIN, M., BERTHON, J.F., KOPELEVICH, O.V. and CAMPBELL, J.W., 2000, Remote sensing of ocean colour in coastal and other optically complex waters, IOCCG Report #3, S. Sathyendranath (Ed.).

SCHLOSS, I.R., FERREYRA, G.A., FERRARIO, M.E., ALMANDOZ, G.O., CODINA, R., BIANCHI, A.A., BALESTRINI, C.F., OCHOA, H.A., RUIZ, P.D. and POISSON, A., 2007, Role of plankton communities in the sea-air variation of pCO_2 in the SW Atlantic Ocean. *Marine Ecology Progress Series*, **332**, pp. 93–106.

SOKAL, R.R. and ROHLF, F.J., 1995, *Biometry: the principles and practice of statistics in biological research*, 3rd ed. (San Francisco, USA: W.H. Freeman).

STRICKLAND, J.D.H. and PARSONS, T.R., 1972, *A Practical Handbook of Seaweater Analysis*, Bulletin 167 (Ottawa, Ontario, Canada: Fisheries Research Board of Canada).

UTERMÖHL, H., 1958, Zur vervollkommnung der quantitativen phytoplankton-methodik. *Mitteilungen der Internationale Vereinigung fur theorestiche und angewandte Limnologie*, **9**, pp. 1–38.

VOLPE, G., SANTOLERI, R., VELLUCCI, V., RIBERA D'ALCALÁ, M., MARULLO, S. and D'ORTENZIO, F., 2007, The colour of the Mediterranean Sea: global versus regional bio-optical algorithms evaluation and implication for satellite chlorophyll estimates. *Remote Sensing of Environment*, **107**, pp. 625–638.